

# Sensitivity of two Component Mode Synthesis Methods Applied to Addition and Subtraction of Substructures

Elizabeth J. Bergman<sup>\*</sup>, Matthew S. Allen<sup>†</sup> &  
*University of Wisconsin-Madison, Department of Engineering Physics*  
*1500 Engineering Drive, Madison, Wisconsin 53706-1609*

Randall L. Mayes<sup>‡</sup>  
*Sandia National Laboratories, P.O. Box 5800, Albuquerque, New Mexico 87185*

Modal substructuring or Component Mode Synthesis (CMS) has been standard practice for many decades in the analytical realm, yet significant difficulties have been encountered when applying CMS with experimentally derived modal models. One well known difficulty is that one cannot measure the usual set of fixed-interface and constraint modes used in the Craig-Bampton method, but this alone does not explain the drastic errors that have been encountered experimentally, especially when seeking to use CMS to remove one substructure from another. This work explores this issue, investigating the effect of mismatch between the subsystem modal model and the experimental system when uncoupling substructures. The Modal Constraints for Fixture and Subsystem (MCFS) method was recently found to reduce the sensitivity of the substructure uncoupling process for a few problems of interest. The conventional approach for uncoupling substructures employs constraints at the physical points at which they are connected, while the MCFS method employs constraints over the entire substructure that are enforced in a least-squares sense. This work compares the sensitivity of the MCFS method and the conventional method to errors in the natural frequencies, damping ratios and mode shapes of the substructures. The methods are compared both analytically and using Monte Carlo simulation. The MCFS method is shown to be less sensitive to uncertainty than the CPT method for the system of interest.

## I. Introduction

Modern space and aircraft structures are typically designed by groups of engineers, each of which is primarily responsible for a particular subsystem. The dynamic performance of the structure usually depends on how all of these subsystems interact, yet some may be very difficult to model adequately. For example, satellites are often comprised of a supporting structure that houses numerous electronic components, thermal management systems, etc... Structural design groups will typically create detailed finite element models of the structure, yet they do not have enough information to adequately model each subcomponent, and are probably not interested in creating and validating detailed models of some subcomponents that are supplied by other groups or by external vendors. In cases such as these, it may be much more efficient to perform tests to experimentally characterize some subcomponents and then to combine an experimentally generated model of the subcomponents to the structural finite element model. This same scenario also presents itself outside of the aerospace industry as well. For example, a company that designs automotive seats is probably not interested in modeling the entire structure of each of the automobiles in which their seats may be used, especially considering the complexity of the automobile due to its intricate geometry, joints with unknown properties, variety of materials, unknown damping effects, and the potential for nonlinearity. However, that structure strongly affects the performance of their seats as experienced by a consumer.

Methods for combining experimental and analytical substructures can be classified in two different groups. Response based methods, such as impedance coupling [1-3] or admittance coupling ([4]), which operate on

---

<sup>\*</sup> Graduate Research Assistant, 534 Engineering Research Building, Member AIAA.

<sup>†</sup> Assistant Professor, 535 Engineering Research Building, [msallen@engr.wisc.edu](mailto:msallen@engr.wisc.edu), Member AIAA.

<sup>‡</sup> Distinguished Member of Technical Staff, Mail Stop 0557.

frequency response matrices of the subsystems to predict the frequency response of the coupled system. The other approach, dubbed Modal Substructuring (MS) or Experimental Component Mode Synthesis (ECMS or CMS) joins the substructures based on their linear differential equations of motion [5, 6]. A few works have compared these two approaches [2, 7, 8]. This work focuses on ECMS, although the methods studied are also applicable to impedance coupling [9], which give the same results under certain circumstances.

Numerous works have studied modal substructuring with regard to finite element analysis. The Craig-Bampton [10] method has enjoyed widespread use and good success in the analytical realm, although other methods have also proven effective in a variety of cases ([11]). Many prior studies have focused on efficient ways in which one can generate modal models of subcomponents, employing the free modes of the substructures, the combination of fixed-interface and constraint modes employed by Craig and Bampton [10], modes with the interfaces mass weighted ([11]), etc... It is generally accepted that free-interface modes are not a very efficient basis for a substructure and that the other methods may improve the accuracy of the total system predictions for the same number of modes. Experimentally, fixed-interface modes cannot be accurately simulated for most structures of interest, so mass-weighted interface modes are often employed [11].

While the modal basis has enjoyed most of the lime-light in the literature, experimental applications of modal substructuring have shown that small errors in the experimentally derived subcomponent models often have a drastic effect on the combined system predictions [2, 12], so these considerations are often much more important to experimental CMS than the particular modal basis employed. This work explores the sensitivity of ECMS to inaccuracies in the subcomponent models, which are inevitable in experimental measurements. ECMS usually requires measurement of the rotation of the connection point so rotational constraints can be enforced. Rotational measurement transducers are still in their infancy, so methods are typically devised to infer the connection point motion. For example, researchers have employed finite different techniques ([1-3]) to estimate rotational motion at the connection points, yet these techniques usually require differences of measurements of similar magnitude, and hence can magnify the uncertainty at the connection point.

One attractive way to estimate rotational motions involves attaching a fixture to the interface of each subcomponent, instrumenting the fixture to deduce its rigid body motion, and then removing the mass of the fixture from the experimental model. Using a fixture, one can increase the separation between measurement transducers to more accurately estimate rotational motion. For example, Figure 2 shows a photograph of a steel beam with a fixture attached. The long beam is the substructure of interest; the fixture was attached to mass load the interface and to facilitate measurement of the rotation motion of the beam at its end. The length of the fixture was chosen to be the minimum that resulted in adequate estimates of the rotational motion of the connection point. A similar technique was employed by Carne, Nelson and Dohrman [4] in the late 1990's for an automotive system. They used the rigid body modes of the fixture, derived from its geometry, to find the six degree-of-freedom connection point motion (displacement and rotation in three directions) from 12 unidirectional accelerometers.

When designing a fixture for a particular application, one cannot always meet the objectives of mass and adequate sensor separation with a fixture that is rigid in the frequency band of interest. Allen and Mayes [7] recently extended this approach to account for the flexibility of an elastic fixture. A modal filter [13] was employed to estimate the motion of the fixture in terms of its rigid body and elastic modal coordinates, from which the rotation and displacement of the connection point (CPT) was deduced. They also presented an alternative method, dubbed the Modal Constraint for Fixture and Subsystem (MCFS) method, which circumvents the use of the physical connection point, and significantly improved the accuracy of their predictions for an experimental substructure comprised of two beams. This method may also provide significant advantages when connecting substructures at multiple points, as initially demonstrated in [9].

Allen and Mayes were not the first to explore substructure un-coupling, or subtraction of one substructure from a structure. Dr. P. Ind explored this issue in his doctoral thesis [12], motivated by the desire to infer the motion of a delicate substructure from response measurements on an elastic fixture and away from the connection point. His work showed progress towards this goal, but that significant development is needed before the procedure can be reliably applied. In some cases, the CMS procedure failed dramatically.

This work explores the sensitivity of the MCFS method, and of ECMS in general, to inaccuracies in the modal parameters of the subsystem models. The initial impetus for the MCFS method is a physical justification, which is verified experimentally for the system of interest in this work. A rigorous uncertainty analysis is also presented, revealing why the MCFS method is more robust than the CPT method for the system of interest. Other unique features of the MCFS method are also discussed. Section II presents the theoretical background. The methods are applied to a simple system in Section III, and conclusions are presented in Section IV.

## II. Modal Substructuring / Component Mode Synthesis Theory – Coupling and Uncoupling

A detailed derivation of component mode synthesis can be found in many works [10, 14]; this work has followed the derivation in Ginsberg [6] which easily accommodates systems where the number of measurement points is vastly different from the system's model order.

Well established methods exist that identify a modal model for a test structure [15, 16], having the following equations of motion

$$\begin{aligned} \{\ddot{q}\} + [\backslash 2\zeta_r \omega_r \backslash] \{\dot{q}\} + [\backslash \omega_r^2 \backslash] \{q\} &= [\Phi]^T \{F\} \\ \{y\} &= [\Phi] \{q\} \\ [\Phi] &= [\{\phi_1\} \quad \dots \quad \{\phi_N\}] \end{aligned} \quad (1),$$

where  $[\backslash 2\zeta_r \omega_r \backslash]$  and  $[\backslash \omega_r^2 \backslash]$  are  $N \times N$  diagonal matrices containing the modal damping constants and modal natural frequencies squared, respectively. The mass normalized mode matrix  $[\Phi]$  is  $N_p \times N$ , where  $N_p$  is the number of physical coordinates  $\{y\}$ , which may be far more, or far fewer than the number of modal degrees of freedom  $N$ . One can easily modify this representation to include the residual flexibility of the truncated modes.

One can join two subsystems by concatenating their modal coordinates, and then defining constraints between them. For example, consider removing a subsystem denoted A from a subsystem C to form subsystem B as illustrated in Figure 1. Let A and C have  $N_A$  and  $N_C$  modes and  $N_{pA}$  and  $N_{pC}$  physical coordinates respectively. The combined equations of motion are

$$\begin{aligned} \begin{bmatrix} -[I_A] & 0 \\ 0 & [I_C] \end{bmatrix} \begin{Bmatrix} \ddot{q}_A \\ \ddot{q}_C \end{Bmatrix} + \begin{bmatrix} -[\backslash 2\zeta_r \omega_r \backslash]_A & 0 \\ 0 & [\backslash 2\zeta_r \omega_r \backslash]_C \end{bmatrix} \begin{Bmatrix} \dot{q}_A \\ \dot{q}_C \end{Bmatrix} + \begin{bmatrix} -[\backslash \omega_r^2 \backslash]_A & 0 \\ 0 & [\backslash \omega_r^2 \backslash]_C \end{bmatrix} \begin{Bmatrix} q_A \\ q_C \end{Bmatrix} &= \\ &= \begin{bmatrix} [\Phi_A]^T & 0 \\ 0 & [\Phi_C]^T \end{bmatrix} \begin{Bmatrix} F_A \\ F_C \end{Bmatrix} \\ \begin{Bmatrix} y_A \\ y_C \end{Bmatrix} &= \begin{bmatrix} [\Phi_A] & 0 \\ 0 & [\Phi_C] \end{bmatrix} \begin{Bmatrix} q_A \\ q_C \end{Bmatrix} \end{aligned} \quad (2),$$

where  $I$  denotes an identity matrix and  $O$  denotes a matrix of zeros of the appropriate dimensions. The A system's matrices are negative, since its mass, stiffness and damping are to be removed from system C.

The previous equation shows two independent systems; one must define constraints between them to arrive at the coupled system. The physical coordinates will typically be joined using linear constraints:

$$[a_p] \begin{Bmatrix} y_A \\ y_C \end{Bmatrix} = \{0\} \quad (3)$$

where  $[a_p]$ 's dimensions are the number of constraint equations times by  $N_{pA} + N_{pC}$ . These in turn couple the modal degrees of freedom  $\{q\}$  as follows

$$[a_p] \begin{bmatrix} [\Phi_A] & 0 \\ 0 & [\Phi_C] \end{bmatrix} \begin{Bmatrix} q_A \\ q_C \end{Bmatrix} = [a] \begin{Bmatrix} q_A \\ q_C \end{Bmatrix} = \{0\} \quad (4).$$

The constraint equations are applied to equation (2) using the methods described in Ginsberg [6], and repeated in the authors' previous publication [7], resulting in a symmetric set of equations of motion for the combined system in terms of the unconstrained generalized coordinates.

The number of degrees of freedom  $\{q\}$  of the combined system should not be confused with the number of physical coordinates. All of the physical coordinates  $\{y\}$  will always be valid, even after enforcing a constraint,

although some of them may be equal to one another due to the constraint. On the other hand, the number of degrees of freedom depends on the sizes of the systems being joined and the number of constraints. If  $N_{CE}$  constraint equations are used, then the combined system will have  $N_C + N_A - N_{CE}$  degrees of freedom. One difference between modal uncoupling and finite element assembly becomes apparent. Suppose A, B and C are finite element models, and that A and B are joined at  $N_{CE}$  nodal degrees of freedom to form system C. The process of coupling systems A and B results in system C having  $N_C = N_A + N_B - N_{CE}$  degrees of freedom. If we then uncouple A from C ( $C-A=B$ ) using the same procedure, we obtain a final system with  $N = N_B + 2*N_A - 2*N_{CE}$  degrees of freedom. This final system should be the B system, yet its size is different from  $N_B$  unless  $N_A$  is equal to  $N_{CE}$ , in other words if each and every node on system A is constrained to the corresponding nodes on system C during the coupling and uncoupling processes. Such an approach may not be practical from an experimental standpoint, so additional degrees of freedom may be present after substructure uncoupling.

### A. Connection Point Constraints (CPT)

Most previous works have considered coupling and uncoupling substructures at the point or points at which they meet physically [11, 17]. Here this is dubbed the Connection Point (CPT) method. This is stated simply as follows,

$$\{y_{CPT}^C\} = \{y_{CPT}^A\} \quad (5),$$

where  $y_{CPT}^C$  and  $y_{CPT}^A$  denote the connection point degrees of freedom on substructures C and A respectively. This can be easily rearranged into the form in equation (3). The number of constraint equations is determined by the number of physical connection degrees of freedom that must be equated to enforce continuity at the point(s) where the substructures meet.

### B. Modal Constraints for Fixture and Subsystem (MCFS)

If the model for the fixture and its negative copy are identical, then one would expect that enforcing the constraint in eq. (5) at one point should cause every point on both the fixture and negative fixture to move in unison. On the other hand, if the fixture and its negative model differ, then their motion might also differ away from the connection point. For example, if their natural frequencies differed, the two fixtures would oscillate at different rates, resulting in a nonzero force at the connection point. From a structural control perspective, it seems that it might be easier to assure that the two fixtures undergo the same motion if we were to monitor the motion and apply control forces at (enforce constraints) at a set of points that are distributed spatially, but this might also be problematic because one could inadvertently command a fixture to move in a direction in which it is very stiff or not capable of moving due to its limited modal basis. This could cause the two fixtures to bind and result in large errors.

Allen and Mayes [7] suggested an approach that circumvents some of these difficulties called Modal Constraints for Fixture and Subsystem (MCFS). As the name implies, the idea is to constrain the modal coordinates of the fixtures. Specifically, the following constraint equations are used

$$[\phi_m^A]^\dagger \{y_m^C\} = [\phi_m^A]^\dagger \{y_m^A\} \quad (6),$$

where  $[\phi_m^A]^\dagger$  denotes the pseudoinverse of the mode matrix for system A. The subscript “m” signifies that this mode matrix is comprised only of the rows corresponding to a set of measurement points on the fixture. The pseudoinverse results in one constraint equation for each mode that is included in  $\phi^A$ . Typically, fewer modes are included than there are sensors so that equality between the displacements  $y_m^C$  and  $y_m^A$  is not strictly enforced. One can then retain both  $y_m^C$  and  $y_m^A$  in the equations of motion for the final system and check whether equality of motion of these points has been adequately enforced. If the motion of these points differs, this may signify inaccuracy in either the fixture model or the test results.

### C. Effect of Uncertainty on CPT and MCFS

Some level of uncertainty is inevitable in the experimentally measured natural frequencies and mode shapes of the component substructures. Errors creep in due to sensor calibration uncertainty, measurement noise and cross-axis sensitivity when accelerometers are employed. Also, continuous substructures can only approximately be represented using a finite number of modes, so some degree of model truncation error is expected.

### 1. Physical Justification

The initial impetus behind employing modal constraints rather than a connection point constraints came from viewing the substructure subtraction process as a structural control problem, as described previously. The connection point method tries to enforce equality of motion between the fixture and its negative model by requiring that both fixtures have the same motion at the connection point. If the fixtures are equivalent, then this is sufficient to ensure that their motion matches at all of the physical points comprising both fixtures. From a control perspective, one point is sufficient to command all of the states of a system if that point renders the system controllable, but one can envision that relatively small mismatch in the two fixture models may result in vastly different motion at points that are far removed from the connection point if the fixture is elastic. Additional inputs may render the system more controllable, or more robust.

The MCFS method constrains the modes, as observed over a number of distributed points, of the two fixtures. Hence, one would expect that the two fixtures should have similar motion, even if their models are different. One can easily check that the two fixtures are moving in unison by retaining the measurement points on each fixture in the final system model. The constraint condition should cause these points to move in unison, so any difference in their motion is indicative of either error in the fixture model or sensitivity of the coupling procedure. This is illustrated in Section III.A.

### 2. Mathematical Comparison of Sensitivity to Uncertainty

The CPT and MCFS strategies differ only in the constraint equations used between the negative analytical fixture and the experimental fixture. Uncertainty in these constraint equations translates into error in the predictions of the combined system responses. A simple model of how this uncertainty propagates is difficult to derive because the mathematical formulas involving the constraint equations are complex, especially if they are reordered using a singular value decomposition if the algorithm in [7] is used to assure good numerical conditioning. Fortunately, one can infer something about the sensitivity of the two methods by simply comparing the sensitivity of their constraint equations, which are given in eqs (5) and (6).

First consider the MCFS method. Recall that the equations of motion exist in modal space, and that the response at any of the locations  $\{y_m\}$  are given by the product of the mode shapes at those locations  $[\phi_m]$  and the modal coordinates. The constraint matrix  $[a_{MCFS}]$  becomes

$$[a_{MCFS}] = \begin{bmatrix} [I] & -[\phi_m^A]^\dagger [\phi_m^C] \end{bmatrix}. \quad (7)$$

The uncertainty in this constraint matrix is a function of the uncertainty in the experimentally measured mode shapes of the C system at the measurement locations. One may also ascribe uncertainty to the A system modes to represent the potential for mismatch between the analytical fixture model and the actual modal properties of the fixture as installed on the test structure.

Uncertainty in the constraint equations employed in the CPT method depends on how the motion of the connection point, possibly including rotational motion, is obtained. If the connection point motion can be measured directly, then the uncertainty is governed by uncertainty in the mode shapes of the C system and the analytical fixture A at the connection point. As discussed previously, one is usually not able to measure the connection point motion directly, particularly the rotational degrees of freedom, so these must be estimated in some way. Finite difference schemes can be employed to measure the connection point rotation, but these are known to amplify errors in test mode shapes because one must often take the difference between two very similar numbers, so one would expect the uncertainty at the connection point to be much larger than the uncertainty elsewhere. In this case the CPT method would be less robust than the MCFS method.

Another way of estimating the connection point motion involves the use of a modal filter, as was done in [7]. (The same basic approach was also used in [18].) One first approximates the motion at a set of measurement points as a sum the fixture's modes as follows

$$\begin{Bmatrix} \{y_m\} \\ \{y_{CPT}\} \end{Bmatrix} = \begin{bmatrix} [\phi_m^A] \\ [\phi_{CPT}^A] \end{bmatrix} \{q\}, \quad (8)$$

where  $\{y_m\}$  denotes a vector of responses at the measurement points,  $\{y_{CPT}\}$  denotes the responses at the connection point,  $[\phi_m]$  and  $[\phi_{CPT}]$  denote the corresponding mode shapes, and  $\{q\}$  is a column vector of modal coordinates. One presumably has an analytical model for the fixture, so the mode shapes are known (or one may use the rigid body mode shapes of the fixture based on geometry as in [18]), then one can solve for the connection point motion.

$$\{y_{CPT}\} = [\phi_{CPT}^A] [\phi_m^A]^\dagger \{y_m\}, \quad (9)$$

This presumes that there are at least as many measurement points as there are modes in the fixture model, and that the measurement points are selected so that  $[\phi_m]$  is well conditioned. Substituting this expression into eq. (6), one obtains the following constraint matrix for the CPT method,

$$[a_{CPT}] = \left[ \begin{array}{c} [\phi_{CPT}^A] \quad -[\phi_{CPT}^A][\phi_m^A]^\dagger [\phi_m^C] \end{array} \right] \quad (10)$$

or,

$$[a_{CPT}] = [\phi_{CPT}^A] [a_{MCFS}]. \quad (11)$$

This constraint matrix is equivalent to the modal constraint matrix premultiplied by  $[\phi_{CPT}^A]$ , so there is a linear relationship between uncertainty in the connection point constraint matrix and the MCFS constraint matrix. Each column of  $[a_{CPT}]$  depends only on the corresponding column of  $[a_{MCFS}]$ , so one can readily compute the relationship between the covariance of  $[a_{CPT}]$  and the covariance of  $[a_{MCFS}]$ ,

$$\text{cov}([a_{CPT}(:,k)]) = [\phi_{CPT}^A] \text{cov}([a_{MCFS}(:,k)]) [\phi_{CPT}^A]^T. \quad (12)$$

$a(:,k)$  denotes the  $k$ th column of matrix  $a$ .

This analysis reveals that the sensitivity of the CPT method may be greater or smaller than that of the MCFS method, depending on whether the connection point fixture mode shapes magnify or decrease uncertainty in eq. (12). The mode shapes of the C system at the measurement points  $[\phi_m^C]$  and the pseudo-inverse of the mode shape matrix of the fixture  $[\phi_m^A]$  influence the MCFS constraint matrix in eq. (7), so both methods will be sensitive to uncertainty in these quantities.

One should observe that the mode shape matrix at the connection point degrees of freedom  $[\phi_{CPT}^A]$  is not necessarily square. For example, consider joining two beams in two dimensions as done in the following section. One must enforce three constraints, two in-plane displacements and one in-plane rotation between the beams, so  $[\phi_{CPT}^A]$  would have three rows. A two-dimensional fixture has three rigid body modes, so employing a rigid fixture would result in  $[\phi_{CPT}^A]$  being square. If the fixture is sufficiently flexible then elastic modes must also be included and  $[\phi_{CPT}^A]$  might have more columns than rows. This was the case in the application in the following section.

### III. Application

This section compares the MCFS and CPT methods both experimentally and numerically. A simple structure was designed to test the CMS procedures, which is comprised of two beams. The 24 in. long Beam D is modeled analytically. Beam B, which is 12 in long, is a substructure that we do not wish to model analytically, so its model will be derived from test. To facilitate measurement of the connection point rotation, and to mass load the interface of the B system modes to obtain a better basis for the substructuring analysis, Fixture A (4.6 in. long) is attached to beam B during the tests, so substructure C, which is the combination of A and B, is the system that is actually tested. Six accelerometers are placed on Fixture A to characterize its motion. An analytical model of Fixture A is developed so its effect can be removed from C. The total substructuring process then includes two steps, first removing A from C to obtain B, and then joining D to B. Subsystem D exists as an analytical model, specifically, an Euler-Bernoulli beam model, whose natural frequencies have been updated to match the frequencies measured on a real beam of the same dimensions. All of the components are made of steel. Beams B and D are 0.75 in. high by 1.0 in. wide; Fixture A's cross section is 1.0 in. by 1.0 in.

In all of the following, A and C will be coupled using both modal constraints and connection point constraints. In either case, D will be connected to the negative fixture A using connection point constraints (A is an analytical model so the connection point rotation is known.) The goal of the substructuring procedure is to correctly determine the frequency response functions of system E between points 1 and 2 in Figure 1.

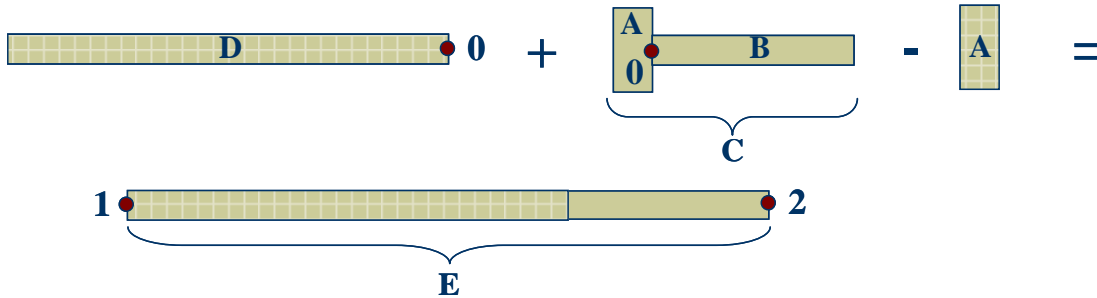


**Figure 1: Test system for Experimental-Analytical substructuring. Experimental model for Beam B is to be joined to analytical Beam D after Fixture A is removed using CMS uncoupling**

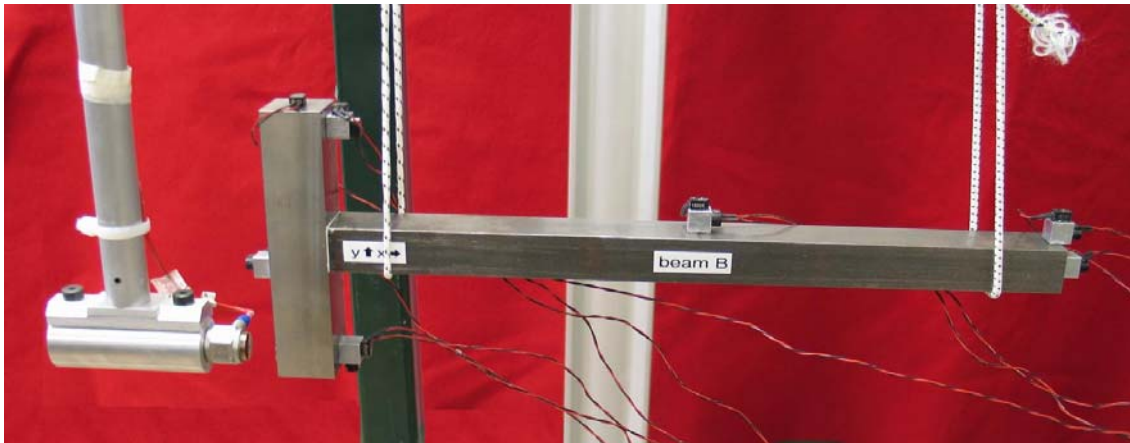


**Figure 2: Photograph of experimental setup for testing Beam B with Fixture A using impact hammer.**

### A. Experimental Application

The T-beam shown in Figure 2 (system C) was tested and six modes were extracted below 9000 Hz. These were supplemented with the analytically derived rigid body modes and used to create a modal model of the T-beam. The analytical fixture (A) was modeled as two guided-free Euler beams, each of whose length was reduced by half of Beam B's thickness to account for the stiffening effect that Beam B has on the fixture. The analytical model for Beam D was described in the previous section. The testing procedures were explained in more detail in [8].

Figure 3 shows the axial FRFs predicted between the measurement points 1 and 2 on the total structure (see Figure 1) using the CPT and MCFS methods. The analytical prediction, tuned to match the modal properties of an actual 36 in. beam, is also shown. Both methods accurately predict the frequency and amplitude of the first axial mode, but the CPT method greatly underestimates the frequency of the second axial mode. Furthermore, the CPT method shows a zero in the FRF near 5800 Hz, which is not reasonable for the combined system because the input and excitation points are on the extreme edges of Beam E. The lateral FRFs found using the CPT and MCFS methods both agreed very closely with the analytical result, as shown in Figure 4.

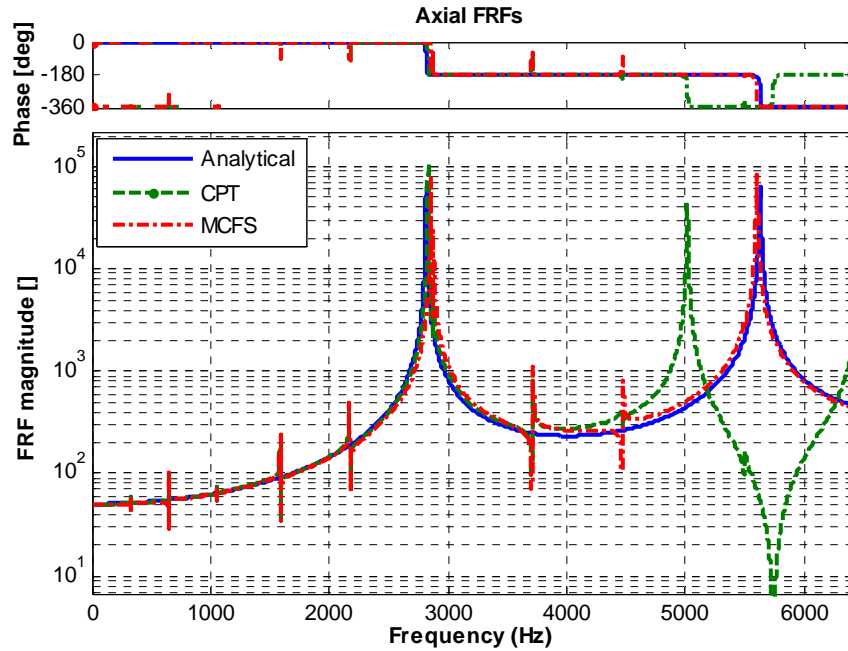


**Figure 3: Axial FRFs between points 1 and 2 of Beam E derived from experimentally measured mode shapes for system C. Lines correspond to Analytical result (solid), MCFS result (dash-dot) and CPT result (dash).**

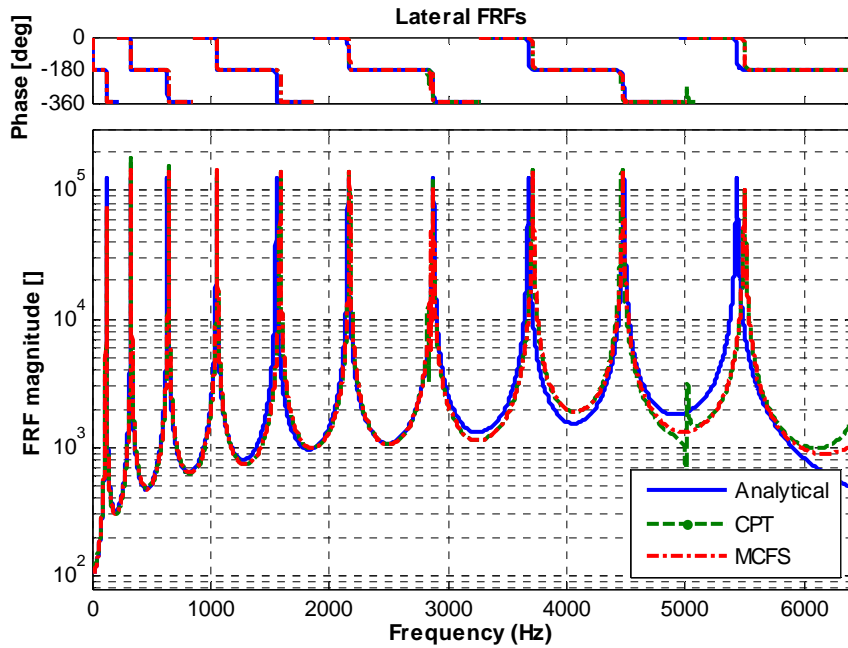


**Figure 4: Lateral FRFs between points 1 and 2 of Beam E derived from experimentally measured mode shapes for system C. Lines correspond to Analytical result (solid), MCFS result (dash-dot) and CPT result (dash).**

Various modifications to the fixture model were explored, and the experimental results were checked and re-checked, but none of these efforts improved the performance of the CPT method for the beam's second axial mode. However, when the CPT method was employed with a rigid fixture model [7] the CPT method predicted two axial modes in the bandwidth of interest and didn't produce a spurious zero in the FRFs, but the predicted frequencies for both axial modes were about 700 Hz too low (due to the fixture's neglected elasticity).

As discussed previously, one can evaluate the effectiveness of the constraint conditions in coupling the negative analytical fixture to the C-system by comparing the motion of the measurement points on both systems for each of the modes of the combined system. This comparison is shown in Figure 5. Blue circles show the locations of the measurement points corresponding to the accelerometers shown in Figure 2. The displacements at each of these points in the first axial mode of vibration are shown with triangles and crosses for systems C (T-beam) and A (fixture) respectively. Note that uniaxial accelerometers were used, so each displacement is in a single direction only. When the MCFS method is used, the motion of the A and C measurement points matches closely, implying that the Modal constraints have effectively enforced equivalent motion between the two systems. On the other hand, the motions differ considerably between A and C for the CPT method. For the second axial mode, the discrepancy was far worse than shown here when CPT constraints were used while no significant differences were observed between the A and C motions for the MCFS method. The motion on the A and C systems matched very closely for all of the bending modes of the E system using either CPT or MCFS constraints. It was also observed that the coupling process accurately predicted the response in the lateral direction when the fixture's flexibility was not included in the model, suggesting that the fixture was essentially rigid for bending motion of system C.

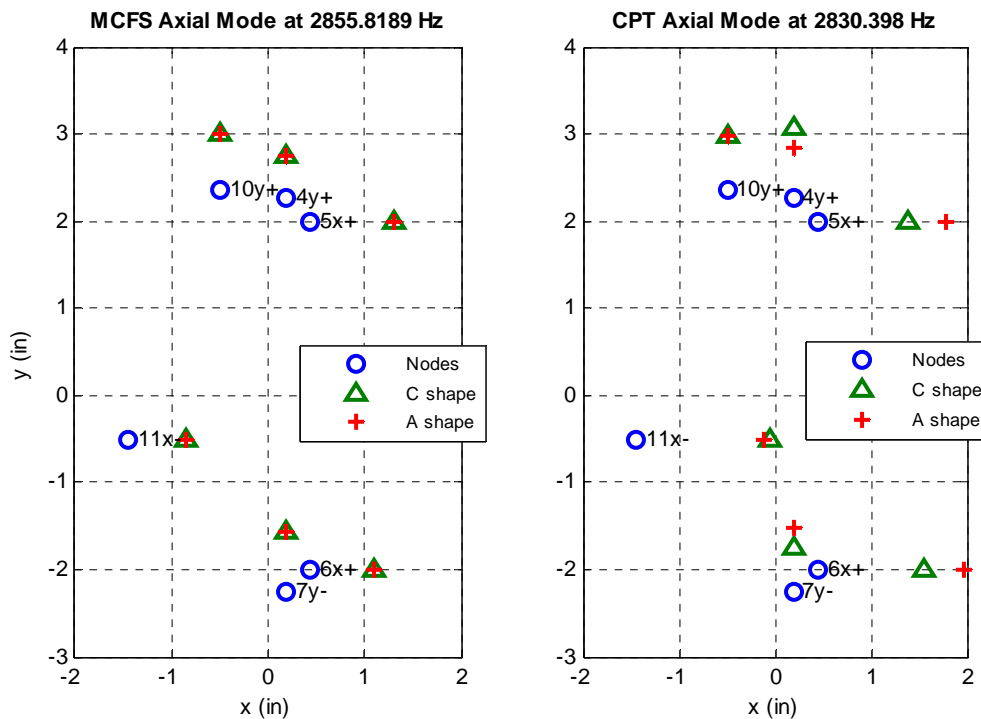


**Figure 5: Mode shapes of 1<sup>st</sup> axial mode found using MCFS and CPT methods at the fixture's measurement points. The mode shape at these points shows the A and C fixtures having nearly the same motion for the MCFS method, while significant difference are observed between the corresponding sensors when the CPT method is used.**

## B. Numerical Application

The goal of substructure coupling is usually to avoid modeling some component of a system. In this section a model for system C is used in order to simulate the substructure coupling process so we may evaluate its sensitivity to measurement noise. Towards this end, a finite element model for the T-beam in Figure 2 was created in NASTRAN. The model is allowed lateral and axial displacement and in-plane rotation. Both the beam and the fixture were made of steel with nominal weight density  $0.28 \text{ lb/in}^3$ , modulus of elasticity  $30e6 \text{ lb/in}^2$ . Each beam is modeled with ten node tetrahedral elements in NASTRAN as shown in Figure 6. The model also includes the accelerometer mounting blocks. There are a total of 6 measurement locations on the fixture (subsystem A) and 2 measurement locations on beam B. Table 1 lists the elastic mode natural frequencies of each subsystem. Figure 7 shows the first bending mode and first axial mode of subsystem C. The first axial mode of the T-beam involves

significant deformation of the fixture, and the pattern is reminiscent of the free elastic mode of the fixture, which is shown in Figure 8.

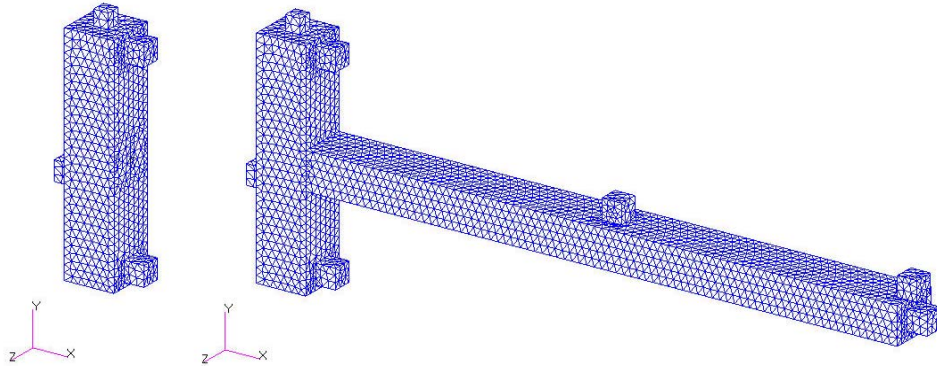


**Figure 6: Solid finite element models of subsystems A (left) and C (right).**

Elastic Mode	Subsystem A (Fixture) Frequency (Hz)	Subsystem C (T-beam) Frequency (Hz)
1	8317.84	665.12
2	18750.54	1617.48
3	21695.55	3115.24
4	29302.70	5175.46
5	35462.79	5399.88
6	38888.49	8330.10
7	43559.55	8597.29

**Table 1: Elastic mode natural frequencies of subsystems A and C**

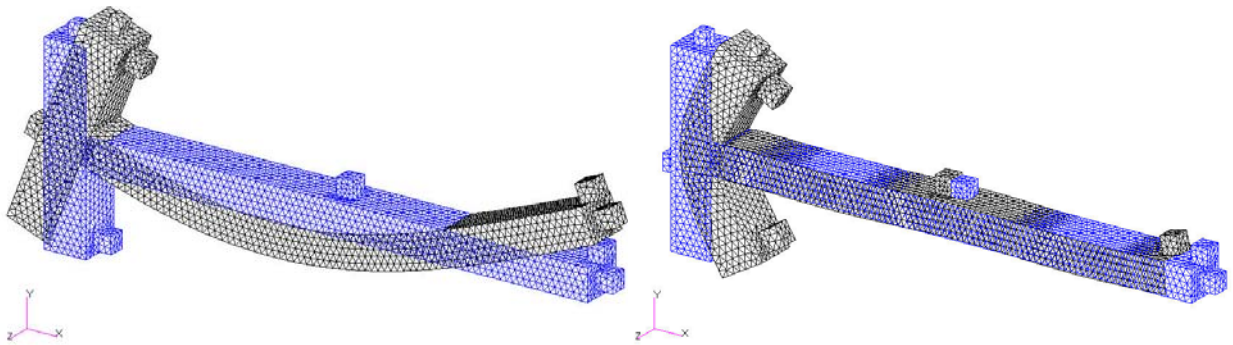


**Figure 7: First bending mode (665.12 Hz, left) and first axial mode (5175.46 Hz, right) of subsystem C.**

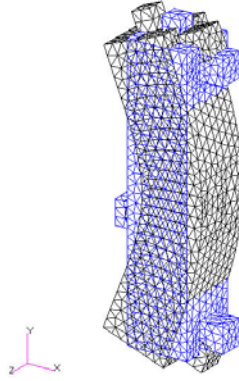


**Figure 8: First elastic mode (8317.84 Hz) of subsystem A.**

The mass normalized mode shapes of each subsystem were truncated to the measurement degrees of freedom that were used experimentally. Only frequencies below 10,000 Hz for subsystem C were used in the analysis. Therefore, a total of ten modes (three rigid body and seven elastic) were used for subsystem C. Three rigid body modes and the first elastic mode of subsystem A (fixture) were used in this analysis. The same analytical model for Beam D was used for this case as was used in the experimental case.

The FEA mode shapes of the C system were compared with those that were obtained experimentally, and found to be in good agreement overall, but significant differences were observed in a few locations. For example, the axial mode shape of the FEA model on the right end of the beam was -0.087, 0.098, 0.304, for modes 4, 5 and 6 respectively. The corresponding experimental mode shapes were -1.84, -1.71, -2.11, at least an order of magnitude larger. It was also noted that the experimental lateral shapes at this location were -20.8, -18.8, -21.3 for those same modes, suggesting that the discrepancy may be a result of cross-axis sensitivity.

The CMS procedure was performed using the truncated FEA models for subsystems A and C. The analytical and simulated FRF's for the MCFS and CPT methods are shown in Figure 9. Neither method matches the analytical result very well, although some of the mismatch could be due to the fact that the FEA frequencies for the C system were about 5% higher than the experimental frequencies, so the Analytical model based on the experimental E system is not perfectly consistent with the result we expect to obtain here. The most surprising observation is that the CPT method once again gives an erroneous prediction of the 2<sup>nd</sup> axial mode, and predicts spurious zeros in the FRF near where that mode should be. This is unexpected because the only errors present in this simulation are model truncation errors; the models for A and C are perfectly consistent as they were derived from the same FEA model. The lateral predictions for the CPT and MCFS methods both agreed closely with the analytical, and are not reproduced here.

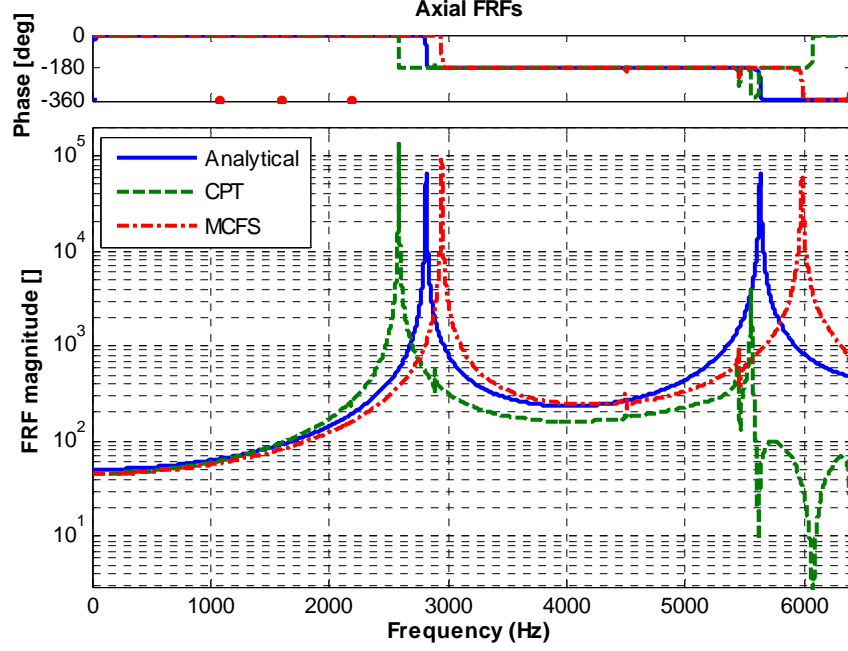


**Figure 9: Axial FRFs between points 1 and 2 of Beam E, using Finite element model mode shapes for Beam C and Fixture A. Lines correspond to Analytical result (solid), MCFS result (dash-dot) and CPT result (dash).**

Our purpose in creating the FEA model was to be able to study the effect of errors in the component models on the CMS process. Figure 9 shows that the CPT method already exhibits substantial error even when experimental error is not present. However, it was hoped that this case would still provide a meaningful comparison of the relative sensitivity of the two methods.

Experimental errors were modeled by introducing random noise into the mode shapes of subsystem C. Uniformly distributed noise was used, scaled such that the noise amplitude for each mode was 5% of the maximum displacement in that mode. A uniform model was employed because it presumes no information about the nature of the noise contaminating the mode shape measurements, except that it is bounded by a certain value. The actual noise profile obtained in a real experiment is much more complicated than that represented here, but this model at least captures the potential for relatively large errors in some sensors due to small signal amplitudes.

$$[\phi]_{\text{exp } C} = [\phi]_{FEMsubC} + [\phi]_{\text{noise}} \quad (13)$$

$$\{\phi\}_{\text{noise}} = n * e * \{U\} \quad (14)$$

where

$[\phi]_{\text{exp } C}$  = Simulated experimental mode shapes of subsystem C

$[\phi]_{FEMsubC}$  = Subsystem C FEM mode shapes

$\{\phi\}_{\text{noise}}$  = vector of noise added to each FEM target mode shape

$n$  = noise level, in this study 5%

$e$  = scaling factor which is equal to the maximum value of each mode shape

$\{U\}$  = vector of uniformly distributed random numbers between -1 and 1.

A Monte Carlo simulation (MCS) was performed by applying this noise profile 100 times to the mode shapes of subsystem C. The covariance of each term in the constraint matrix  $[a]$  was estimated from the MCS. Before doing this, one must note that the constraint equation is homogenous, so each row of  $[a]$  could be multiplied by an arbitrary constant, while preserving the same constraint matrix. Hence, the rows of  $[a]$  were first normalized so they would have a maximum value of unity before computing the statistics on  $[a]$ . As was noted previously, each column of  $[a]$  is independent of all others, so the statistics can be computed column by column. Table 2 displays the

maximum value and the mean absolute value of the covariance between all combinations of the terms in  $[a]$ . The connection point method's covariances that are 20-50 times larger than the MCFS method, so it appears that it is more sensitive to errors in the experimental mode shapes than the MCFS method.

	MCFS	CPT
<b>max cov[a]</b>	0.0069	0.28
<b>mean  cov[a] </b>	2.53E-5	9.51E-4

**Table 2: Covariances of Constraint Matrix for MCFS and CPT**

The lateral and axial FRFs were also computed at each trial in the MCS. The resulting FRFs in the axial direction are displayed in Figures 10 and 11. Blue lines show the analytical FRF in the axial direction. A red line is shown for each trial of the MCS. As seen in Figure 10, the MCFS method consistently predicts two axial modes in the vicinity of the analytical axial modes. However, it also produces erroneous results between 0 and 1000 Hz, which seem to be artificial coupling between the bending and axial motions of the beam. The CPT method, shown in Figure 11, fails to produce the correct qualitative result for any of the 100 MCS trials. It also shows very large variation in the low-frequency mass-line.

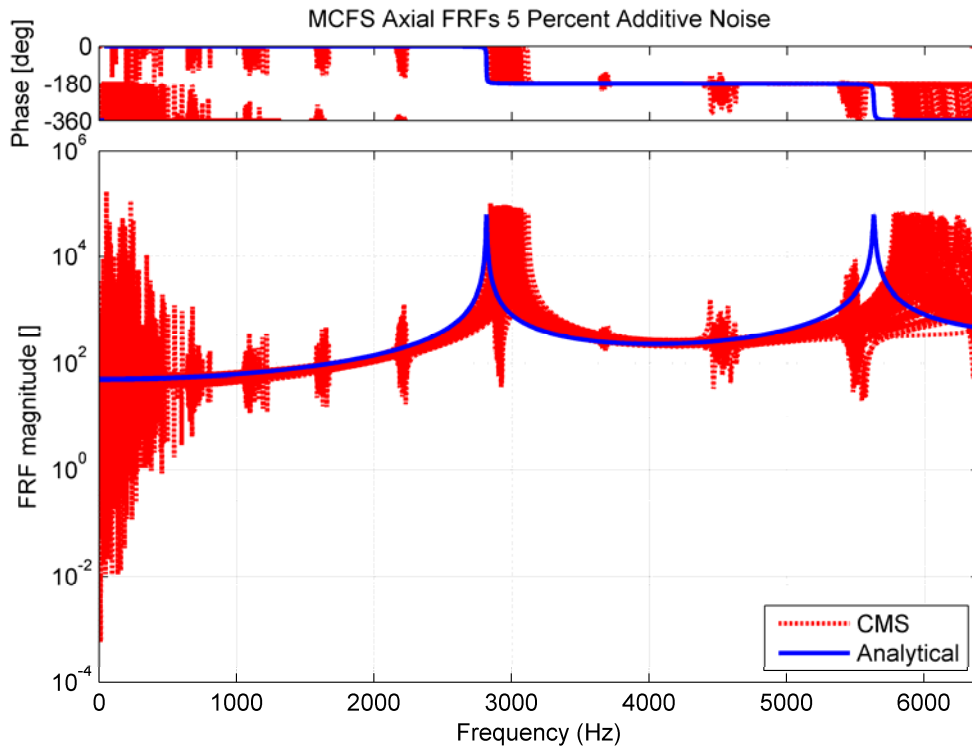


**Figure 10: Analytical axial FRF and CMS result for 100 iterations of the Monte Carlo simulation, using MCFS to remove subsystem A.**

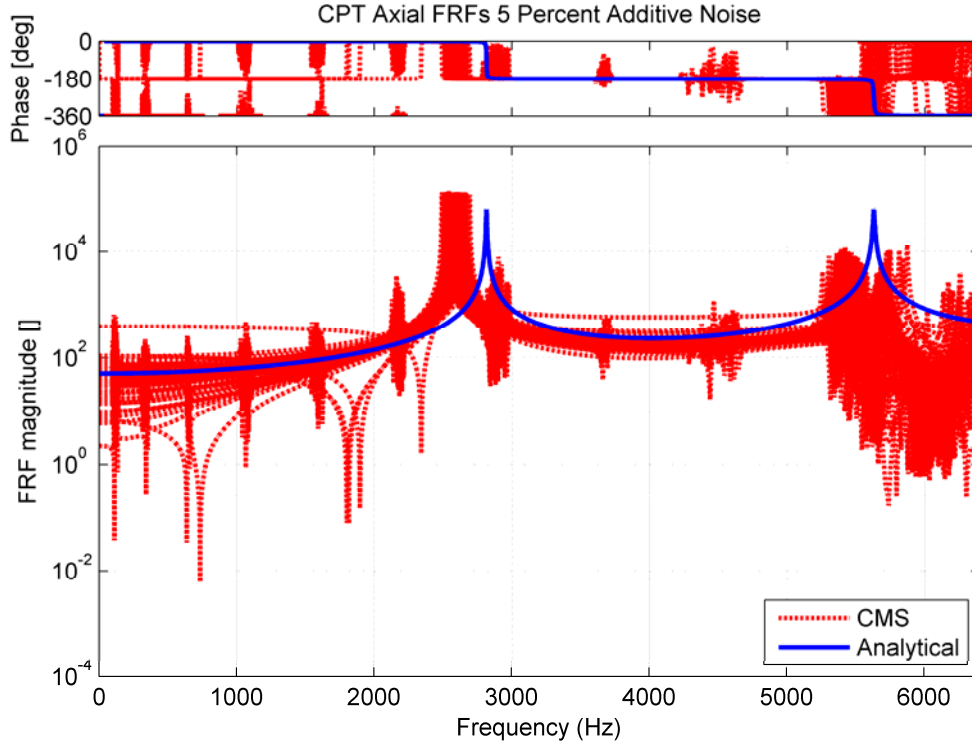


**Figure 11: Analytical axial FRF and CMS result for 100 iterations of the Monte Carlo simulation, using CPT constraints to remove subsystem A.**

#### IV. Conclusions

When performing substructure coupling between experimental and analytical models, it is often beneficial to employ a fixture at the substructure interfaces during the experimental tests. A fixture facilitates accurate measurement of the rotational motions at the interface and can also mass-load the interface, thus improving the modal database for the subcomponent. However, the effects of the fixture must be removed in the substructuring process, and this process can be sensitive to experimental errors, especially if the fixture's flexibility contributes to the subcomponent's motion.

Two methods were presented by which a fixture can be removed from the experimentally derived model for a subcomponent. Both employ a modal filter to characterize the motion of the fixture when attached to the experimental substructure. The first method, dubbed the connection point method (CPT) multiplies the modal response by the connection point mode shapes of the fixture to estimate the connection point motion. A negative fixture is then coupled to the positive fixture at the connection point to remove its effect from the experimental substructure. The second method, dubbed the Modal Constraint for Fixture and Subsystem (MCFS), simply equates the modal degrees of freedom of the fixture to the corresponding motion on the physical fixture. This latter approach is preferred physically, because it enforces equality of motion between the fixture and its negative model at all points over the fixture, whereas the CPT method enforces equality at a single point and relies on equivalence between the negative fixture model and the actual fixture to ensure that the spatial motion of the fixtures is the same. Mathematically, it is shown that the CPT constraint equations are equal to the MCFS constraint equations multiplied by the connection point mode shapes.

The MCFS and CPT methods were applied using a modal data base for system C comprised of experimentally measured mode shapes, frequencies and damping ratios. The MCFS and CPT methods were found to give similar results for the bending modes of the combined system (E), and the MCFS method accurately predicted both axial modes as well, but the CPT method gave wildly inaccurate predictions at higher frequencies. The difficulty stems from the fact that elastic motion of the fixture is important for the axial modes. The CPT method enforces only three constraints to assure that the motion over the entire fixture and its negative model match. This approach proved to be highly sensitive to measurement errors and/or model mismatch. On the other hand, the MCFS method employs a modal filter to constrain the modes of the negative fixture to their representation on system C over a number of spatially distributed points. The motion of the positive and negative fixture was observed for MCFS and

CPT, demonstrating that the MCFS method more accurately enforced equality of motion at the measurement points than did the CPT method.

An analytical model of system C and a highly consistent model for system A were created using Finite Elements. The CMS method was employed using analytical models for C and A. Once again, it was found that the CPT method did not accurately predict the axial motion of the beam, even in the absence of any measurement errors. The nature of the error in the CPT predictions was similar to those that were observed experimentally. A Monte Carlo simulation revealed that the covariance of the constraint matrix for the CPT method was 20 to 50 times that of the MCFS method, once again highlighting the improved sensitivity of the MCFS method.

### Acknowledgments

This work was supported by, and some of this work was performed at Sandia National Laboratories. Sandia is a multi-program laboratory operated by Sandia Corporation, a Lockheed Martin Company, for the United States Department of Energy's National Nuclear Security Administration under Contract DE-AC04-94AL85000.

### References

- [1] M. Imregun, D. A. Robb, and D. J. Ewins, "Structural Modification and Coupling Dynamic Analysis Using Measured FRF Data," in *5th International Modal Analysis Conference (IMAC V)*, London, England, 1987.
- [2] A. P. V. Urgueira, "Dynamic Analysis of Coupled Structures Using Experimental Data," in *Imperial College of Science, Technology and Medicine* London: University of London, 1989.
- [3] T.-J. Su and J.-N. Juang, "Substructure System Identification and Synthesis," *Journal of Guidance Control and Dynamics*, vol. 17, 1994.
- [4] T. G. Carne and C. R. Dohrmann, "Improving Experimental Frequency Response Function Matrices for Admittance Modeling," in *24th International Modal Analysis Conference (IMAC XXIV)*, St. Louis, Missouri, 2006.
- [5] D. R. Martinez, T. G. Carne, D. L. Gregory, and A. K. Miller, "Combined Experimental/Analytical Modeling Using Component Mode Synthesis," Palm Springs, CA, USA, 1984, pp. 140-152.
- [6] J. H. Ginsberg, *Mechanical and Structural Vibrations*, First ed. New York: John Wiley and Sons, 2001.
- [7] M. S. Allen and R. L. Mayes, "Comparison of FRF and Modal Methods for Combining Experimental and Analytical Substructures," in *25th International Modal Analysis Conference (IMAC XXV)*, Orlando, Florida, 2007.
- [8] R. L. Mayes and E. C. Stasiunas, "Lightly Damped Experimental Substructures for Combining with Analytical Substructures," in *25th International Modal Analysis Conference (IMAC XXV)*, Orlando, Florida, 2007.
- [9] R. L. Mayes, P. S. Hunter, T. W. Simmermacher, and M. S. Allen, "Combining Experimental and Analytical Substructures with Multiple Connections," in *26th International Modal Analysis Conference (IMAC XXVI)*, Orlando, Florida, 2008.
- [10] R. R. J. Craig and M. C. C. Bampton, "Coupling of Substructures Using Component Mode Synthesis," *AIAA Journal*, vol. 6, pp. 1313-1319, 1968.
- [11] K. O. Chandler and M. L. Tinker, "General mass-additive method for component mode synthesis," Kissimmee, FL, USA, 1997, pp. 93-103.
- [12] P. Ind, "The Non-Intrusive Modal Testing of Delicate and Critical Structures," in *Imperial College of Science, Technology & Medicine* London: University of London, 2004.
- [13] Q. Zhang, R. J. Allemang, and D. L. Brown, "Modal Filter: Concept and Applications," in *8th International Modal Analysis Conference (IMAC VIII)*, Kissimmee, Florida, 1990, pp. 487-496.
- [14] R. R. J. Craig, *Structural Dynamics*. New York: John Wiley and Sons, 1981.
- [15] D. J. Ewins, *Modal Testing: Theory, Practice and Application*. Baldock, England: Research Studies Press, 2000.
- [16] S. Maia, J. M. M. Silva, J. He, N. A. Lieven, R. M. Lin, G. W. Skingle, W. M. To, and A. P. V. Urgueira, *Theoretical and Experimental Modal Analysis*. Taunton, Somerset, England: Research Studies Press Ltd., 1997.
- [17] D. R. Martinez, A. K. Miller, and T. G. Carne, "Combined Experimental and Analytical Modeling of Shell/Payload Structures," in *The Joint ASCE/ASME Mechanics Conference*, Albuquerque, NM, 1985, pp. 167-194.
- [18] D. de Klerk, D. J. Rixen, S. N. Voormeeren, and F. Pasteuning, "Solving the RDoF Problem in Experimental Dynamic Substructuring," in *26th International Modal Analysis Conference (IMAC XXVI)* Orlando, Florida, 2008.